

Enhanced woody biomass production in a mature temperate forest under elevated CO₂

Received: 11 January 2024

Accepted: 10 July 2024

Published online: 12 August 2024

 Check for updates

Richard J. Norby ^{1,2,3} ✉, Neil J. Loader ⁴, Carolina Mayoral ^{1,5}, Sami Ullah ^{1,2}, Giulio Curioni ^{1,10}, Andy R. Smith⁶, Michaela K. Reay ^{1,2,11}, Klaske van Wijngaarden ^{1,2,7}, Muhammad Shoaib Amjad^{1,12}, Deanne Brettle ^{1,2}, Martha E. Crockatt ^{8,13}, Gael Denny¹, Robert T. Grzesik ^{1,2}, R. Liz Hamilton ^{1,2}, Kris M. Hart ¹, Iain P. Hartley ⁹, Alan G. Jones ^{8,14}, Angeliki Kourmouli ^{1,2,15}, Joshua R. Larsen ^{1,2}, Zongbo Shi ^{1,2}, Rick M. Thomas ^{1,2,16} & A. Robert MacKenzie ^{1,2} ✉

Enhanced CO₂ assimilation by forests as atmospheric CO₂ concentration rises could slow the rate of CO₂ increase if the assimilated carbon is allocated to long-lived biomass. Experiments in young tree plantations support a CO₂ fertilization effect as atmospheric CO₂ continues to increase. Uncertainty exists, however, as to whether older, more mature forests retain the capacity to respond to elevated CO₂. Here, aided by tree-ring analysis and canopy laser scanning, we show that a 180-year-old *Quercus robur* L. woodland in central England increased the production of woody biomass when exposed to free-air CO₂ enrichment (FACE) for 7 years. Further, elevated CO₂ increased exudation of carbon from fine roots into the soil with likely effects on nutrient cycles. The increase in tree growth and allocation to long-lived woody biomass demonstrated here substantiates the major role for mature temperate forests in climate change mitigation.

Carbon uptake and storage by terrestrial vegetation is a major source of uncertainty in projections of future levels of CO₂ in the atmosphere and the resulting effects on climate^{1,2}. Multiple lines of evidence indicate that increasing atmospheric CO₂ concentration in recent decades resulting from anthropogenic emissions and land use change have led to higher rates of CO₂ uptake by plants, that is, the CO₂ fertilization effect, including in forests, which dominate the terrestrial C cycle^{3,4}. Evidence for forest responses to the atmospheric CO₂ concentrations that will be attained in future decades comes from a limited number of

decade-long free-air CO₂ enrichment (FACE) experiments in which forest plots were exposed to elevated CO₂ (eCO₂). These 'first generation' forest FACE experiments^{5–7} were established in young tree plantations, and questions arise as to the extent to which their responses to eCO₂, including increased growth and primary productivity, are predictive of the responses of older, more established forests^{8–10}. There are multiple issues to consider. As forests develop over time, nitrogen, which is often the limiting resource in unmanaged temperate stands, becomes increasingly sequestered in wood or recalcitrant soil organic matter

¹Birmingham Institute of Forest Research, University of Birmingham, Edgbaston, UK. ²School of Geography, Earth & Environmental Sciences, University of Birmingham, Edgbaston, UK. ³Environmental Sciences Division, Oak Ridge National Laboratory, Oak Ridge, TN, USA. ⁴Department of Geography, Swansea University, Swansea, UK. ⁵School of Biosciences, University of Birmingham, Edgbaston, UK. ⁶School of Environmental and Natural Sciences, Bangor University, Bangor, UK. ⁷Hawkesbury Institute for the Environment, Western Sydney University, Penrith, New South Wales, Australia. ⁸Earthwatch Europe, Mayfield House, Oxford, UK. ⁹Geography, Faculty of Science, Environment and Economy, University of Exeter, Exeter, UK. ¹⁰Present address: Forest Research, Northern Research Station, Roslin, UK. ¹¹Present address: Organic Geochemistry Unit, School of Chemistry, University of Bristol, Bristol, UK. ¹²Present address: Department of Botany, Women University of Azad Jammu and Kashmir Bagh, Bagh, Pakistan. ¹³Present address: Leverhulme Centre for Nature Recovery, School of Geography and the Environment, University of Oxford, Oxford, UK. ¹⁴Present address: Scion, Rotorua, New Zealand. ¹⁵Present address: Lancaster Environment Centre, Lancaster University, Bailrigg, Lancaster, UK. ¹⁶Present address: Big Sky Science Ltd., West Midlands, UK. ✉e-mail: RNorby@utk.edu; a.r.mackenzie@bham.ac.uk

and unavailable to support plant growth, a phenomenon referred to as progressive nitrogen limitation (PNL)^{11–13}. Furthermore, the development of PNL can be accelerated by eCO₂ (ref. 14). PNL is of particular interest today because global atmospheric carbon and nitrogen sources are now moving in opposite directions^{15,16}. Phosphorus limitation might be a critical influence on responses to eCO₂ on sites with old, highly weathered soils^{9,17}. Apart from nutrient limitations, older trees may be less responsive to eCO₂ than younger trees because a smaller fraction of the biomass is live tissue contributing to growth.

The amount of biomass produced each year—the net primary productivity (NPP)—is a key metric for evaluating forest response to eCO₂ and a benchmark for models^{18–20}. If NPP increases in eCO₂, the key question becomes whether the additional C accumulates in wood or instead is allocated to leaves and fine roots that turn over rapidly and release the C back to the atmosphere²¹. Carbon allocated to wood can persist in the ecosystem for policy-relevant time frames^{22,23}, which provides negative feedback to atmospheric CO₂. Over longer time frames and landscape scales, C sequestration depends not just on the effects of eCO₂ on tree growth but also on the rate of tree mortality¹⁰, and some evidence suggests that increased growth rate may shorten a tree's lifespan^{24,25}. Nevertheless, the effect of rising CO₂ on NPP and how it is allocated, as revealed in FACE experiments, is critical input to any evaluation of the interaction between terrestrial ecosystems and atmospheric CO₂.

A common question being addressed across the 'second generation' forest FACE experiments is whether mature forests will respond to eCO₂ (ref. 9). Although the definition of 'mature' in this context is vague²⁶, the new or developing FACE experiments in the Amazon forest in Brazil (<https://amazonface.unicamp.br/>), a Eucalyptus stand in Australia¹⁷ and a temperate maritime oak forest at the Birmingham Institute of Forest Research (BIFoR) in central England, UK^{27,28}, are in forest stands that are centuries or more older than the young plantations in the ORNL FACE¹⁴ and DukeFACE experiments²⁹ in southeastern United States. For example, the ORNL FACE and BIFoR FACE are both in temperate deciduous forests (albeit with different species) that had attained canopy closure, linear growth and reproductive maturity; however, the *Quercus robur* trees that dominate in BIFoR FACE are ~180 years old compared with the 10–20-year-old *Liquidambar styraciflua* trees in ORNL FACE, and the stand structure is very different—similar tree basal area per plot (34 cm² m⁻²) is concentrated in 5–7 trees per plot at BIFoR (average tree basal area of 3,486 cm²) compared with 90 trees at ORNL FACE (average tree basal area of 118 cm²) (ref. 30). Here we address whether this difference in age and stand structure precludes the response of tree growth to eCO₂ at BIFoR FACE.

BIFoR FACE facility

The BIFoR FACE facility (<https://www.birmingham.ac.uk/research/bifor/face/index.aspx>, Extended Data Fig. 1) is located in central England (52.801° N, 2.301° W, 107 m above sea level). The 19 ha Mill Haft deciduous forest woodland was established as a plantation of oak 'standards' (that is, timber trees) with hazel coppice in the mid-nineteenth century and has been very lightly managed since that time, the understory hazel trees being last coppiced in ~1985. About two thirds of the 400 ha estate surrounding Mill Haft were arable and pasture until 2010, since when they have been converted into mixed broadleaf plantation and no-till organic herbal ley (a mixture of grasses, legumes and herbs) in roughly equal proportion³¹. The forest is dominated by 180-year-old *Quercus robur* L. trees, which represent 92% of the forest's basal area. The forest canopy is 24–26 m high with a leaf area index of the overstorey of ~6. The forest understory comprises *Corylus avellana* L. coppice, *Acer pseudoplatanus* L., *Crataegus monogyna* Jacq. and a few individuals of other broadleaf species³². The dominant soil is Dystric Cambisol with a sandy-clay texture. Underlying geology is a Helsby sandstone formation. Mean annual maximum and minimum temperatures (1991–2020) were 13.5 and 6.0 °C with 676 mm precipitation³³. The FACE facility

comprises six experimental arrays surrounding plots of ~30 m diameter. Disturbance to the woodland was avoided during construction of the FACE infrastructure, fitting the infrastructure between the trees so that no oak standards or coppice stools were removed and using no concrete foundations or guy wires²⁷. CO₂-enriched air (1–2% by volume) was released from vertical vent pipes in three of the arrays to attain a target CO₂ concentration at plot centre that is 150 ppm above ambient CO₂. Actual daytime CO₂ concentration enrichment during the 2017–2022 growing seasons (April–November) was 140 ± 38 ppm relative to ambient air due to occasional disruptions in CO₂ supply. Full description of the FACE facility and its operating characteristics are available²⁷.

Aboveground biomass production

Evaluation of treatment effects required accounting for pretreatment differences among plots. Tree-ring analysis (see Methods) revealed high variability in the size and growth of the 180-year-old *Q. robur* trees on plots within the experimental arrays (Fig. 1a), as is often typical of mature forest stands; this variability complicates detection of possible effects of eCO₂ while underlining the realism of the BIFoR FACE context and increasing its applicability to other real-world forests. Furthermore, basal area increment (BAI) in plots randomly assigned to receive eCO₂ starting in 2017 was significantly greater than in plots for ambient CO₂ (aCO₂) before the initiation of the CO₂ treatment (Fig. 1b). Hence, these pretreatment differences were accounted for in evaluating treatment differences after eCO₂ exposure was initiated. We used the average plot-specific BAI from 2011–2015 (based on tree-ring analysis) to normalize subsequent annual growth data, thereby accounting for site and stand differences that would otherwise obscure treatment effects. A departure in the normalized tree-ring chronologies between aCO₂ and eCO₂ plots was apparent beginning in 2017, the first year of eCO₂ exposure (Fig. 1c).

It has become clear that application of published allometric equations for temperate forests can create considerable errors in biomass estimation when applied to a different site with a different stand structure than that from which the relationship was established³⁴. Therefore, we developed a site-specific allometry (Extended Data Fig. 2) on the basis of a terrestrial laser scan (TLS) of the site to calculate annual wood production from diameter measurements (see Methods). TLS provides highly accurate estimates of tree volume that are translated into estimates of aboveground biomass as long as internal stem damage is not large³⁵ and tree cores did not indicate any internal stem damage. Annual diameter increments as measured in the field with manual dendrometers and calipers were consistent with independent measures using automated dendrometers that measure circumference changes continuously (Extended Data Fig. 3) and with the tree-ring chronologies. Dry matter increment (DMI) per tree, as calculated from diameter and adjusted by pretreatment differences among plots, was greater in eCO₂ than in aCO₂ for every year of CO₂ enrichment except for 2019 (Fig. 2); over the 7 years of treatment, tree growth was 9.8% greater in eCO₂. The loss of response in 2019 may have been related to differential defoliation by the winter moth (*Operophtera brumata* L.) and other foliar feeding insects, which was greater in eCO₂ based on litter trap collections³⁶ (Extended Data Fig. 4). There was also an insect outbreak in 2018, which was not seen in the litter collection data and had no apparent effect on the growth response. Although the apparent difference in DMI in any year was not statistically significant, repeated measures analysis indicated a significant CO₂ effect over the 2017–2023 period ($P = 0.028$, $F_{1,4} = 5.48$). Total DMI over the experimental period was linearly related to tree size (basal area), with no clear discontinuities in the relationship or in the distribution of ambient vs elevated trees around the distribution (Extended Data Fig. 5).

Net primary productivity

With additional data on fine-root and leaf mass production, understory production, reproductive output and exudation (see Methods),

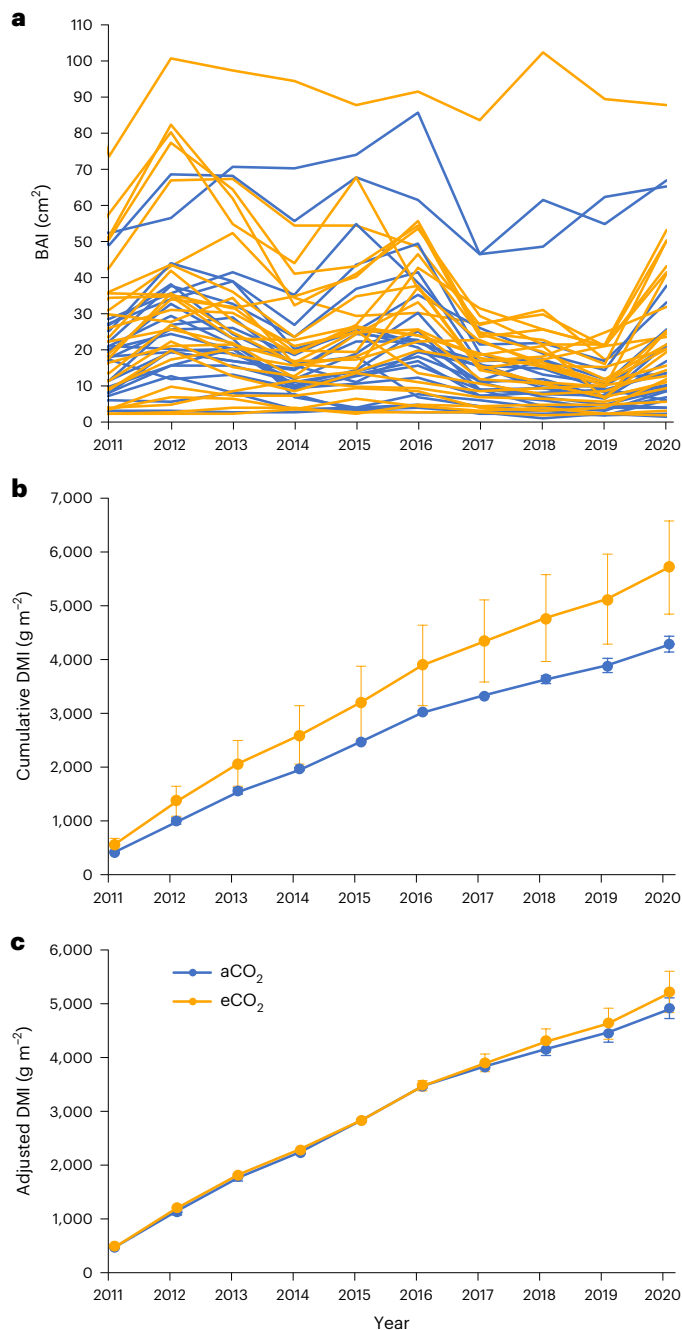


Fig. 1 | Tree-ring chronologies of *Quercus robur* L. trees in the FACE experimental plots. a, Annual BAI of each tree. Orange lines are trees that began receiving elevated CO_2 in 2017; blue lines are trees that remained in ambient CO_2 . **b**, Cumulative DMI per plot area since 2010; data are the means of trees in three ambient CO_2 plots and three elevated CO_2 plots \pm s.e. **c**, Cumulative DMI adjusted by dividing data in **b** by the mean DMI from 2011 to 2015 relative to the overall mean for the period.

NPP and its response to eCO_2 were estimated for 2021 and 2022, the 5th and 6th years of eCO_2 treatment (Table 1). Aboveground *Q. robur* wood production comprised the largest fraction (40–48%) of NPP, followed by leaf production and fine-root production. After accounting for pretreatment differences in wood and leaf production, total NPP was 9.7% greater in eCO_2 in 2021 and 11.5% greater in 2022, but neither of these differences were statistically significant ($P > 0.20$). Given the variance structure of the forest stand in the six plots, a CO_2 enhancement of 45% would have been required in a given year to achieve

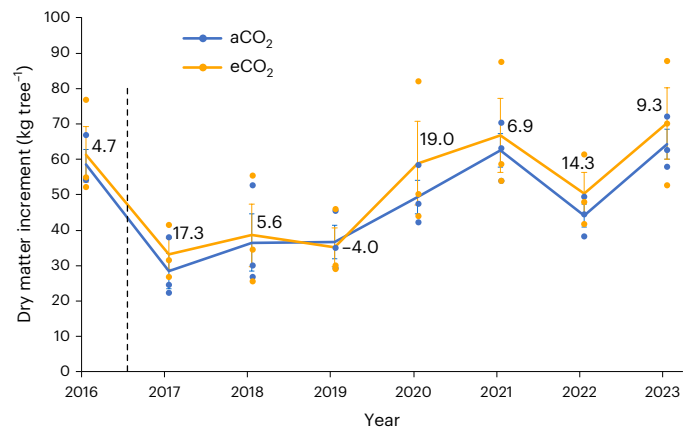


Fig. 2 | Dry matter increment per tree. Data are the mean \pm s.e. of trees in three plots each in ambient CO_2 (blue) and elevated CO_2 (orange). Numbers above the points represent the percentage increase (or decrease) in eCO_2 relative to aCO_2 . CO_2 exposure began in 2017; pretreatment (2016) data calculated from tree-ring analysis. Repeated measures analysis of variance indicated that the effect of CO_2 was significant at $P = 0.0279$, $F_{1,24} = 5.48$; $\text{CO}_2 \times \text{year}$ was not significant ($P = 0.830$, $F_{6,24} = 0.46$).

a statistically significant ($P < 0.05$) difference, greatly exceeding what has been observed in previous forest FACE experiments⁵. Alternatively, given the measured means and variance, 28 arrays per treatment would have been required to achieve type I and II errors of 0.05 and 0.20. Taking the 2 years together in a repeated measures framework, NPP increased 10.6% ($P = 0.099$, $F_{1,4} = 4.56$), equivalent to -1.7 tonnes dry matter per hectare per year.

Most of the observed increase in NPP was attributable to wood production; there was no difference in fine-root or leaf mass production, although standing stock of fine roots may have been greater and turnover slower in eCO_2 . Leaf mass per unit area (LMA) was -10% greater and oak leaf area index (LAI) was 5% less in eCO_2 (Table 2). LAI in fully occupied sites with relatively high LAI is not expected to increase in eCO_2 (ref. 37). Significant increases in fine-root production are common in forest FACE experiments³⁷ but have mainly been observed as a response to eCO_2 in nutrient-limited forest ecosystems³⁸. Although increased fine-root production was reported from measurements predominantly under stools of coppiced *C. avellana* in years 1 and 2 of the BIFoR FACE CO_2 treatment³⁹, the absence of a sustained increase in the BIFoR experiment is not unexpected, given that the BIFoR FACE forest does not appear to be N-limited (discussed further below). Nevertheless, there was evidence of increased carbon allocation belowground as exudation. Exudation of organic carbon from roots is a component of NPP but is rarely included in estimates, given the difficulty in measuring and upscaling exudation. We measured rates of net exudation four times between August 2020 and June 2021 (see Methods) and scaled data expressed as grams C per unit root mass to grams dry mass equivalent per m^2 land on the basis of fine-root mass per unit area from soil cores collected in 2021 and 2022; we assumed that exudation rate in the organic horizon applied equally to deeper roots and that the average of four measurements in spring, summer and autumn reflected the average exudation rate during the 264-day growing season. Exudation flux was 63% greater in eCO_2 in 2021 ($P = 0.13$) and 43% greater in 2022 ($P > 0.20$); repeated measures analysis indicated a significant overall effect ($P = 0.042$, $F_{1,4} = 8.64$).

Discussion

The responses observed in FACE experiments require careful consideration of temporal and spatial scales and levels of biological complexity before their implications for the global carbon cycle and feedbacks to

Table 1 | Net primary productivity and its fractional distribution

	<i>Q. roburbole</i> + branch	<i>Q. roburcoarse</i> root	Understory wood	Total wood	Fine root	Exudation	Reprod.tissue	Leaves	Total NPP
2021	NPP (g m ⁻²)								
Ambient	755±95	83±12	12±7	849±103	203±28	76±20	124±13	501±9	1,753±114
Elevated	835±166	88±21	15±7	938±183	201±11	124±15	133±31	529±49	1,924±263
E/A	1.106	1.060	1.269	1.104	0.989	1.633	1.075	1.054	1.097
2022									
Ambient	534±67	58±8	16±1	608±74	154±8	83±8	72±1	562±22	1,479±78
Elevated	621±87	67±10	17±10	706±87	156±15	118±25	95±28	575±88	1,650±140
E/A	1.164	1.141	1.087	1.161	1.014	1.426	1.318	1.023	1.115
2021	Fractional distribution (%)								
Ambient				48.1±2.7	11.6±1.7	4.2±0.8	7.2±1.1	28.8±1.9	
Elevated				47.8±4.7	10.8±1.5	6.5±0.4	6.9±1.2	27.9±1.6	
E/A				0.995	0.929	1.542	0.967	0.967	
2022									
Ambient				40.8±2.8	10.5±0.9	5.6±0.3	4.9±0.3	38.2±2.2	
Elevated				42.7±3.8	9.5±1.0	7.2±1.6	6.1±2.0	34.5±2.5	
E/A				1.045	0.908	1.174	1.243	0.904	

All data are the means of three plots in ambient CO₂ and three plots in elevated CO₂ ±s.e., expressed as grams dry matter per m². None of the differences within year are statistically significant ($P > 0.20$); repeated measures analysis across years indicated an effect of CO₂ on NPP at $P = 0.099$, $F_{1,4} = 4.56$. Wood production by plot was adjusted to account for the average pretreatment BAI for 2011–2015 as determined by tree-ring analysis. Leaf mass production was assumed to be 14% greater than litter mass based on the amount of nitrogen resorbed from senescing leaves and the assumption that nitrogen was exported as glutamine³⁰. Plot-level leaf mass production was normalized to the pretreatment (2016) values. Production of fine roots (<2 mm diameter) was determined from in-growth cores installed to 30 cm depth and scaled to 1 m depth on the basis of the relative depth distribution of fine-root standing crop in core samples. E/A is the ratio of the measure in eCO₂ to the measure in aCO₂.

Table 2 | Leaf area index, calculated from litter mass and green leaf mass per unit area and adjusted to pretreatment (2016) values

CO ₂ treatment	2020	2021	2022
Litter mass (g m ⁻² land)			
Ambient	330±28	291±19	358±21
Elevated	348±20	332±5	392±23
E/A	1.053	1.139	1.093
LMA (g m ⁻² leaf)			
Ambient	66.5±5.5	60.0±2.6	60.1±0.7
Elevated	73.3±9.8	67.3±1.8	64.2±5.5
E/A	1.102	1.121	1.068
LAI (m ² m ⁻²)			
Ambient	6.02±0.47	5.85±0.38	7.16±0.22
Elevated	5.65±0.94	5.51±0.94	6.85±0.96
E/A	0.939	0.941	0.956

Green leaf mass is assumed to equal litter mass ×1.14 (ref. 30). All data are means ±s.e. of three plots per treatment. No differences are significant ($P > 0.20$) except litter mass and LMA in 2021 ($P = 0.110$, $F_{1,4} = 4.2$ and $P < 0.082$, $F_{1,4} = 5.33$, respectively). E/A is the ratio of the value in eCO₂ to the value in aCO₂.

climate change can be properly interpreted. Forest responses to eCO₂ start with an enhancement of leaf-level photosynthesis, as has been documented at BIFoR FACE³². In many forest systems, the enhancement of photosynthesis scales up to increased NPP⁴, although nutrient limitations can inhibit the translation of increased photosynthesis to increased NPP¹⁷. At BIFoR FACE there is evidence of increased NPP in eCO₂ over 2 years, a response that may become statistically more compelling if it is sustained for more years. It has long been recognized that although NPP might be enhanced by eCO₂ in most terrestrial

ecosystems, a more important question is whether an eCO₂ response results in greater wood mass or instead is allocated to fast-turnover pools (for example, leaves and fine roots)²¹. Aboveground woody biomass is the component of NPP that is most relevant for decades-long (and policy relevant) carbon balance evaluations and the basis of evaluations of past responses to eCO₂. Much of the carbon allocated to wood (other than that in small cast-off branches) will persist in the ecosystem for many decades, whereas much of the carbon allocated to the fast-turnover tissues will quickly return to the atmosphere, although leaf and fine-root necromass also contribute to recalcitrant soil organic matter. At BIFoR FACE, additional carbon taken up in response to eCO₂ through the stimulation of leaf-level photosynthesis³² accumulated in wood, with no increases observed in production of leaves and fine roots. Long-term C sequestration is also determined by tree turnover²⁵, which cannot be assessed at the scale of FACE experiments, but model simulations coupled with inventory analysis in unmanaged temperate forests demonstrated that enhanced tree growth increases biomass stocks despite simultaneous decreases in carbon residence time and tree longevity¹⁰.

Our results contrast with those of EucFACE, where no increases in dry matter accumulation or NPP were observed¹⁷. BIFoR FACE results argue against a general conclusion that older, mature forest systems have no capacity for response to eCO₂. The difference in response between these two experiments is more likely related to nutrient dynamics rather than simply stand age or maturity. EucFACE responses are thought to be limited by a phosphorus deficiency¹⁷, and mature northern temperate forests are generally thought to be nitrogen limited. However, no clear nitrogen or phosphorus limitation has yet been documented at BIFoR FACE, and leaf nitrogen content has been maintained⁴⁰, although further investigation—and indeed further CO₂ treatment—could change these assessments. As a result of surrounding agricultural activities and regional industry, nitrogen deposition at the BIFoR FACE site is relatively high at 22 kg ha⁻¹ (ref. 41) and not atypical of northern temperate forests. This subsidy of reactive nitrogen may

be providing sufficient nitrogen supply to support increased carbon fixation. Furthermore, enhanced soil nitrogen transformations⁴² supported by increased release of bioavailable carbon from root exudation, may be allowing the trees to meet their nitrogen demand under eCO₂. Although exudation comprised just 4–7% of total NPP, this flux of highly labile organic C is disproportionately important to ecosystem biogeochemistry. For example, exudation can increase the availability of labile C, priming the microbial community and associated nitrogen and phosphorus cycling^{43,44}. Measurements on site have shown that net nitrogen mineralization increased on average by 30% under elevated eCO₂, delivering an extra 24 kg N ha⁻¹ yr⁻¹ (ref. 45). However, it is possible that the supply of bioavailable nitrogen sourced from decomposition of soil organic matter may be reduced and eventually exhausted over time. Furthermore, nitrogen deposition is declining in the UK¹⁵ and throughout the Global North⁴⁶. Although at present nitrogen does not appear to be a limiting factor to tree growth or response to eCO₂, nitrogen limitation may develop at BIFoR FACE as the nitrogen cycle gets tighter and plant demand increases, as was observed in a previous FACE experiment¹⁴. Furthermore, high rates of N deposition have been shown to stimulate P acquisition and alleviate potential P limitation⁴⁷, so it is possible that if N deposition declines, P limitation could develop over time.

These BIFoR FACE results have illustrated the importance of and challenges in documenting meaningful ecosystem-scale responses to eCO₂ in mature forests that are inevitably heterogeneous in tree size, productivity and spatial distribution, and in experiments in which engineering constraints limit plot size and financial constraints limit replication and duration. Employing multidecadal tree-ring analysis to account for plot differences before the onset of the CO₂ treatment markedly improved our confidence in attribution of eCO₂ effects. A single year of observation is unlikely to provide convincing evidence of a tree growth or NPP response of the expected possible magnitude; sustained and consistent response over multiple years is necessary. Assessment of dry matter increment is highly dependent on the allometric relationship used to scale non-destructive measurements of tree diameter to biomass. A harvest of trees at the experimental site is precluded, as it is in most forest FACE experiments. Reliance on published allometric equations developed in forests with different stand structures can introduce significant uncertainty in assessment of forest carbon stocks³⁴ and is especially problematic for larger, more mature stands. The development of site-specific allometry developed from non-destructive estimates of *Q. robur* tree volume using terrestrial laser scanning significantly increased our confidence in the assessment of tree biomass in BIFoR FACE.

Our results directly refute the notion that mature forests cannot respond to eCO₂, and they emphasize that the important issue is allocation of any increased carbon uptake and the turnover of the tissues that benefit most²¹. Hence, the evidence from BIFoR FACE of a significant increase in woody biomass production is a key result supporting the role of mature forest stands as decadal C stores¹⁰ and, hence, as natural climate solutions in the coming decades while society undertakes deep decarbonization⁴⁸. Quantifying the CO₂ fertilization effect is important for predictions of future atmospheric CO₂ concentrations and the policy decision that derive therefrom, but even if the increase in tree growth translates to a longer-term increase in C storage in the ecosystem, CO₂ fertilization cannot be seen as reason to delay reductions in fossil fuel consumption.

Online content

Any methods, additional references, Nature Portfolio reporting summaries, source data, extended data, supplementary information, acknowledgements, peer review information; details of author contributions and competing interests; and statements of data and code availability are available at <https://doi.org/10.1038/s41558-024-02090-3>.

References

- Arora, V. K. et al. Carbon-concentration and carbon-climate feedbacks in CMIP6 models and their comparison to CMIP5 models. *Biogeosciences* **17**, 4173–4222 (2020).
- Friedlingstein, P. et al. Uncertainties in CMIP5 climate projections due to carbon cycle feedbacks. *J. Clim.* **27**, 511–526 (2014).
- Schimel, D., Stephens, B. B. & Fisher, J. B. Effect of increasing CO₂ on the terrestrial carbon cycle. *Proc. Natl Acad. Sci. USA* **112**, 436–441 (2015).
- Walker, A. P. et al. Integrating the evidence for a terrestrial carbon sink caused by increasing atmospheric CO₂. *New Phytol.* **229**, 2413–2445 (2021).
- Norby, R. J. et al. Forest response to elevated CO₂ is conserved across a broad range of productivity. *Proc. Natl Acad. Sci. USA* **102**, 18052–18056 (2005).
- Free-Air CO₂ Enrichment Experiments: Results, Lessons, And Legacy* (US Department of Energy, 2020).
- Medlyn, B. E. et al. Using ecosystem experiments to improve vegetation models. *Nat. Clim. Change* **5**, 528–534 (2015).
- Körner, C. et al. Carbon flux and growth in mature deciduous forest trees exposed to elevated CO₂. *Science* **309**, 1360–1362 (2005).
- Norby, R. J. et al. Model-data synthesis for the next generation of forest free-air CO₂ enrichment (FACE) experiments. *New Phytol.* **209**, 17–28 (2016).
- Marqués, L. et al. Tree growth enhancement drives a persistent biomass gain in unmanaged temperate forests. *AGU Adv.* **4**, e2022AV000859 (2023).
- Comins, H. N. & McMurtrie, R. E. Long-term response of nutrient-limited forests to CO₂ enrichment—equilibrium behavior of plant-soil models. *Ecol. Appl.* **3**, 666–681 (1993).
- Johnson, D. W. Progressive N limitation in forests: review and implications for long-term responses to elevated CO₂. *Ecology* **87**, 64–75 (2006).
- Luo, Y. et al. Progressive nitrogen limitation of ecosystem responses to rising atmospheric carbon dioxide. *Bioscience* **54**, 731–739 (2004).
- Norby, R. J., Warren, J. M., Iversen, C. M., Medlyn, B. E. & McMurtrie, R. E. CO₂ enhancement of forest productivity constrained by limited nitrogen availability. *Proc. Natl Acad. Sci. USA* **107**, 19368–19373 (2010).
- Fernández-Martínez, M. et al. Atmospheric deposition, CO₂, and change in the land carbon sink. *Sci. Rep.* **7**, 9632 (2017).
- Tipping, E. et al. Long-term increases in soil carbon due to ecosystem fertilization by atmospheric nitrogen deposition demonstrated by regional-scale modelling and observations. *Sci. Rep.* **7**, 1890 (2017).
- Jiang, M. K. et al. The fate of carbon in a mature forest under carbon dioxide enrichment. *Nature* **580**, 227–231 (2020).
- Hickler, T. et al. CO₂ fertilization in temperate FACE experiments not representative of boreal and tropical forests. *Glob. Change Biol.* **14**, 1531–1542 (2008).
- Walker, A. P. et al. Comprehensive ecosystem model-data synthesis using multiple data sets at two temperate forest free-air CO₂ enrichment experiments: model performance at ambient CO₂ concentration. *J. Geophys. Res. Biogeosci.* **119**, 937–964 (2014).
- Haverd, V. et al. Higher than expected CO₂ fertilization inferred from leaf to global observations. *Glob. Change Biol.* **26**, 2390–2402 (2020).
- Strain, B. & Bazzaz, F. in *CO₂ and Plants: The Response of Plants to Rising Levels of Atmospheric Carbon Dioxide* (ed. Lemon, E. R.) 177–222 (Westview, 1983).
- McCarroll, D. & Loader, N. J. Stable isotopes in tree rings. *Quat. Sci. Rev.* **23**, 771–801 (2004).

23. Walker, A. P. et al. Decadal biomass increment in early secondary succession woody ecosystems is increased by CO₂ enrichment. *Nat. Commun.* **10**, 454 (2019).
24. Brienen, R. J. W. et al. Forest carbon sink neutralized by pervasive growth-lifespan trade-offs. *Nat. Commun.* **11**, 4241 (2020).
25. Körner, C. A matter of tree longevity. *Science* **355**, 130–131 (2017).
26. Martin, P. et al. Can we set a global threshold age to define mature forests? *PeerJ* **4**, e1595 (2016).
27. Hart, K. M. et al. Characteristics of free air carbon dioxide enrichment of a northern temperate mature forest. *Glob. Change Biol.* **26**, 1023–1037 (2020).
28. MacKenzie, A. R. et al. BIFoR FACE: water-soil-vegetation-atmosphere data from a temperate deciduous forest catchment, including under elevated CO₂. *Hydrol. Process.* **35**, e14096 (2021).
29. McCarthy, H. R. et al. Re-assessment of plant carbon dynamics at the Duke free-air CO₂ enrichment site: interactions of atmospheric CO₂ with nitrogen and water availability over stand development. *New Phytol.* **185**, 514–528 (2010).
30. Norby, R. J. et al. Forest stand and canopy development unaltered by 12 years of CO₂ enrichment. *Tree Physiol.* **42**, 428–440 (2021).
31. Bradwell, A. R. *Norbury Park: An Estate Tackling Climate Change* (Norbury Park Estate, 2022).
32. Gardner, A., Ellsworth, D. S., Crous, K. Y., Pritchard, J. & MacKenzie, A. R. Is photosynthetic enhancement sustained through three years of elevated CO₂ exposure in 175-year-old *Quercus robur*? *Tree Physiol.* **42**, 130–144 (2022).
33. *The CEDA Archive* (CEDA, 2023).
34. Calders, K. et al. Laser scanning reveals potential underestimation of biomass carbon in temperate forest. *Ecol. Solut. Evid.* **3**, e12197 (2022).
35. Calvert, J. et al. Modelling internal stem damage in savanna trees: error in aboveground biomass with terrestrial laser scanning and allometry. *Methods Ecol. Evol.* <https://doi.org/10.1111/2041-210X.14375> (2024).
36. Mayoral, C. et al. Elevated CO₂ does not improve seedling performance in a naturally regenerated oak woodland exposed to biotic stressors. *Front. For. Glob. Change* **6**, 1278409 (2023).
37. Norby, R. J. & Zak, D. R. Ecological lessons from Free-Air CO₂ Enrichment (FACE) experiments. *Annu. Rev. Ecol. Evol. Syst.* **42**, 181–203 (2011).
38. Iversen, C. M. Digging deeper: fine-root responses to rising atmospheric CO₂ concentration in forested ecosystems. *New Phytol.* **186**, 346–357 (2010).
39. Ziegler, C. et al. Quantification and uncertainty of root growth stimulation by elevated CO₂ in a mature temperate deciduous forest. *Sci. Total Environ.* **854**, 158661 (2023).
40. Gardner, A., Ellsworth, D. S., Pritchard, J. & MacKenzie, A. R. Are chlorophyll concentrations and nitrogen across the vertical canopy profile affected by elevated CO₂ in mature *Quercus* trees? *Trees Struct. Funct.* **36**, 1797–1809 (2022).
41. Tomlinson, S. J., Carnell, E. J., Dore, A. J. & Dragosits, U. Nitrogen deposition in the UK at 1 km resolution from 1990 to 2017. *Earth Syst. Sci. Data* **13**, 4677–4692 (2021).
42. Sgouridis, F. et al. Stimulation of soil gross nitrogen transformations and nitrous oxide emission under free air CO₂ enrichment in a mature temperate oak forest at BIFoR-FACE. *Soil Biol. Biochem.* **184**, 109072 (2023).
43. Dijkstra, F. A., Carrillo, Y., Pendall, E. & Morgan, J. A. Rhizosphere priming: a nutrient perspective. *Front. Microbiol.* **4**, 216 (2013).
44. Hoosbeek, M. R. et al. More new carbon in the mineral soil of a poplar plantation under Free Air Carbon Enrichment (POPFACE): cause of increased priming effect? *Glob. Biogeochem. Cycles* **18**, GB1040 (2004).
45. Rumeau, M. et al. Nitrogen cycling in forest soils under elevated CO₂: response of a key soil nutrient to climate change. *EGU General Assembly 2022* <https://doi.org/10.5194/egusphere-egu22-178> (2022).
46. Jia, Y. et al. Global inorganic nitrogen dry deposition inferred from ground- and space-based measurements. *Sci. Rep.* **6**, 19810 (2016).
47. Jones, A. G. & Power, S. A. Field-scale evaluation of effects of nitrogen deposition on the functioning of heathland ecosystems. *J. Ecol.* **100**, 331–342 (2012).
48. National Academies of Sciences, Engineering, and Medicine. *Deployment of Deep Decarbonization Technologies: Proceedings of a Workshop* (The National Academies Press, 2019).

Publisher's note Springer Nature remains neutral with regard to jurisdictional claims in published maps and institutional affiliations.

Open Access This article is licensed under a Creative Commons Attribution 4.0 International License, which permits use, sharing, adaptation, distribution and reproduction in any medium or format, as long as you give appropriate credit to the original author(s) and the source, provide a link to the Creative Commons licence, and indicate if changes were made. The images or other third party material in this article are included in the article's Creative Commons licence, unless indicated otherwise in a credit line to the material. If material is not included in the article's Creative Commons licence and your intended use is not permitted by statutory regulation or exceeds the permitted use, you will need to obtain permission directly from the copyright holder. To view a copy of this licence, visit <http://creativecommons.org/licenses/by/4.0/>.

© The Author(s) 2024

Methods

Wood production

Every tree with greater than 10 cm diameter at breast height (DBH) within the array of vent pipes was fitted with a dendroband⁴⁹ at 1.3 m height, or as close as possible to 1.3 m as necessary to avoid a large branch or stem abnormality. Forty-three trees were outfitted in 2016 and five trees were fitted in later years. The initial tree diameter (D) and initial offset of the dendroband were recorded, and the dendroband offset was measured approximately bimonthly between early spring (before leaf out) and late autumn with digital calipers. Diameter and basal area increments (BAI; $BA = \pi \times (D/2)^2$) were calculated from the change in circumference and initial diameter.

Previous analysis of tree biomass at this site employed a published allometric equation for *Q. robur* from ref. 50, which was based primarily on trees harvested in northwestern Spain. This approach was not considered reliable because the largest tree in that data set was smaller than 49% of the BIFoR FACE *Q. robur* trees. Instead, we established a site-specific allometry on the basis of terrestrial laser scans (TLS). Three-dimensional point clouds of the forest stands were collected within the six experimental arrays in January and February 2022, when canopy was in leaf-off condition, using a RIEGL VZ-400i laser scanner (RIEGL Laser Measurement Systems). Registration of separate scans was done in the RiScanPro software (RIEGL) and manual extraction of single trees from the co-registered point cloud was done in CloudCompare (<https://www.cloudcompare.org/>). Determining appropriate parameters for, and the construction of, the Quantitative Structure Models (QSMs) with subsequent calculation of component volumes was done using the open-source software of optQSM (<https://github.com/apburt/optqsm>) and TreeQSM, v.2.4.1 (<https://github.com/InverseTampere/TreeQSM>), respectively. The optimal cylinder model per tree was selected on the basis of the lowest point model distance out of the five iterations. Tree volume was calculated as the sum of bole and branch volume, and volume was converted to dry mass using a wood density of 0.58, an average of trunk and branch density reported for *Q. robur*⁵¹. The regression of $\ln(\text{biomass, kg})$ vs $\ln(\text{diameter, cm})$, with diameter being that calculated from dendroband measurements in December 2021 is: $\ln(\text{biomass, kg}) = 2.312 \times \ln(\text{diameter, cm}) - 1.0863$; $r^2 = 0.77$ (Extended Data Fig. 2).

Aboveground wood mass (kg) of other species was calculated using allometric equations from ref. 50, where M_{stem} is dry matter (kg) and D is diameter (cm):

$$\text{For } \textit{Acer pseudoplatanus}, \ln(M_{\text{stem}}) = -2.3116 + 2.4186 \times \ln(D) \quad (1)$$

$$\text{For other species : } \ln(M_{\text{stem}}) = -2.1653 + 2.4143 \times \ln(D) \quad (2)$$

Annual wood production per tree was calculated as the dry matter increment (DMI) during the year.

Coarse root production for understory species was calculated similarly using the equation⁵⁰:

$$\ln(M_{\text{root}}) = -2.6183 + 2.1353 \times \ln(D) \quad (3)$$

The equation⁵⁰ for *Q. robur* coarse root biomass [$\ln(M_{\text{root}}) = -2.863 + 2.208 \times \ln(D)$] is assumed to be inaccurate to the same extent as the difference between the equivalent aboveground equation⁵⁰ [$\ln(M_{\text{stem}}) = -2.9128 + 2.7442 \times \ln(D)$] and the site-specific TLS-based allometry (Extended Data Fig. 2), which varied from 56% greater to 40% less. Hence, *Q. robur* coarse root biomass was calculated by multiplying aboveground biomass (from the TLS allometry) by the ratio of coarse root to aboveground biomass from the published⁵⁰ equations.

DMI of the multistemmed stools of coppiced *Corylus avellana* was determined by measuring the five thickest sprouts on each hazel stool within the plots irrespective of whether their DBH was below 10 cm, as described⁵². Coarse root production of *C. avellana* was not estimated

as a function of D but was assumed to be 26% of aboveground wood production, as determined from the other understory species.

DMI of the *Q. robur* trees and understory species was expressed per m^2 by dividing total DMI by plot area. The area of the plots, which were not circular to avoid removing large trees during construction, was determined as the area of an irregular polygon with the vertices set to maintain at least a 2.5 m buffer from any vent pipe in the experimental array. The resulting areas as determined with ArcGIS ranged from 574 m^2 to 678 m^2 . DMI was adjusted for pretreatment differences using tree core analysis as described below.

Tree-ring analysis

Increment cores (~4 mm diameter) were collected from the *Q. robur* trees to provide a pretreatment time series of BAI. Cores were collected in June 2021 and August 2022 from the south side of the tree at ~1.3 m height. The cores were stored temporarily in straws and air dried before preparation and ring width measurement. The cores were surfaced using progressively finer grades of abrasive paper to reveal the ring boundaries. Ring widths were measured under magnification using TSAP-Win software (Rinntech) to 1/100 mm. The series were measured in duplicate and internally cross-matched. Tree diameter (not including bark) from 2019 to 2010 was back calculated by sequentially subtracting ($2 \times$ ring width) from each year's calculated diameter, starting with the measured diameter in 2020 minus ($2 \times$ average bark thickness). BAI from 2011 to 2020 was then calculated as the annual increase in BA, with $BA = \pi D^2/4$. To account for pretreatment differences in tree growth across the six plots, the total BAI of each tree from 2011 to 2015 was averaged for each plot, and the relative difference from the overall average BAI for 2011–2015 was used to normalize the data between plots to the site average pretreatment level. The BAI calculated from ring width analysis was on average 15% less than BAI from dendrobands. This is probably because the dendrobands that integrate information on the entire tree circumference are subject to moisture-dependent fluctuations in tree volume and include measures of inner and outer bark thickness, which were not included in the ring width analysis of the air-dried cores.

Leaf production

Leaf production was determined from leaf litter mass. Leaf litter was collected in two or three 1 m^2 traps per plot (2016–2020) and six 0.25 m^2 traps (2020–2022). Litter was collected monthly from March to October and weekly from mid-October to mid-December, separated by species, oven dried and weighed. Some leaves were retained on the trees and fell during the winter and early spring. Hence, annual litter mass production was calculated as the litter collected from April through March. Leaf production exceeds litter mass because of resorption of N-rich organic compounds during senescence. On the basis of the difference in N concentration between green leaves and litter and assuming N is resorbed as glutamate, green leaf production was set to be 14% greater than litter production. Leaf production in 2017–2021 was relativized to pretreatment (2016) values to account for spatial differences.

Flower and fruit production

Flowers and fruit were collected from the litter baskets as described above, dried and weighed. This material comprised flowers, enlarged cups (that is, cups with visible premature acorns), immature acorns, fully mature acorns, empty cups (that is, empty acorn cups without acorns) and galls (acorn development prevented by insect attack).

Fine-root production

Fine-root production was measured from in-growth cores. Five $5 \text{ cm} \times 30 \text{ cm}$ (diameter \times length) mesh columns filled with root-free soil from the O horizon (0–7 cm depth, 0.64 g cm^{-3}), A horizon (7–16 cm depth, 1.03 g cm^{-3}) and B horizon (16–30 cm depth, 1.30 g cm^{-3}) were installed in each plot. Cores were retrieved and replaced every 4–5 months. Fine roots (<2 mm diameter) were removed from the soil,

oven dried and weighed. To extend the fine-root production from the 30 cm deep cores to 1 m depth, adjacent soil cores were collected to 1 m depth and fine-root mass quantified. Production in in-growth cores was extended to 1 m on the basis of the fraction of total fine-root standing crop in the top 30 cm (~65%).

Exudation

Root exudation was measured four times between August 2020 and June 2021. *Q. robur* roots in the O horizon were identified on the basis of surveys of root morphology outside of experimental arrays. Root boxes within 1 m of *Q. robur* trees were installed to permit access to new root growth during this period, and exudates were collected from six root systems per plot. The collection procedure was adapted from ref. 53. Roots (<2 mm diameter) were washed with a nutrient solution (carbon free, NH_4NO_3 40 mg l⁻¹; KH_2PO_4 13.6 mg l⁻¹; K_2SO_4 349 mg l⁻¹; CaCl_2 441 mg l⁻¹ and $\text{MgSO}_4 \cdot 7\text{H}_2\text{O}$ 0.3705 g l⁻¹) to remove adhered soil and placed in a glass syringe filled with glass beads (750 µm) and nutrient solution (10 ml) to mimic the soil environment. Roots were allowed to recover for 48 h, then the nutrient solution was replaced (carbon and nitrogen free, KH_2PO_4 13.6 mg l⁻¹; K_2SO_4 349 mg l⁻¹; CaCl_2 441 mg l⁻¹ and $\text{MgSO}_4 \cdot 7\text{H}_2\text{O}$ 0.3705 g l⁻¹). Exudates were collected for 24 h and the nutrient solution was analysed for dissolved organic carbon content (Shimadzu TOC-L Organic Carbon Analyzer, LOD 0.01 mg C l⁻¹). Roots were dried (40 °C for 48 h) to determine dry mass. Net exudation per gram of dry root per m² was calculated using fine-root standing stock from soil cores ($n = 5$) collected within 1–2 weeks of the exudate collections. To support inclusion of exudation in the calculation of NPP, mass of carbon in exudates was converted to equivalent dry matter units assuming a carbon content of 48%, and the rate per day was scaled to a 246-day growing season. Fine-root mass measured in soil cores sampled in 2022 was used to scale the exudation rates for 2022.

Statistics

Statistical analyses were performed with Stata software. The effect of CO₂ on dry matter increment from 2017 to 2023 was analysed by repeated measures analysis of variance, with plot as the experimental unit and year as the repeated measure. Individual years and the total over the treatment years were analysed using two-sided *t*-test. NPP was analysed similarly, except that only 2 years were included in the repeated measures analysis. The Stata command for repeated measures analysis of DMI (and similarly for NPP) was: `anova dmi co2 plot|co2 year year#co2`.

Reporting summary

Further information on research design is available in the Nature Portfolio Reporting Summary linked to this article.

Data availability

All data are publicly available without restriction at Dryad (<https://datadryad.org/stash>) at <https://doi.org/10.5061/dryad.z612jm6jw> (ref. 54). Biological samples (leaf litter, tree cores) were collected at the BIFoR research site (52.801° N, 2.301° W) and are archived at the University of Birmingham.

Code availability

Quantitative structure models and calculation of tree volume from TLS data (QSMs) used the open-source software optQSM (<https://github.com/apburt/optqsm>) and TreeQSM v.2.4.1 (<https://github.com/InverseTampere/TreeQSM>).

References

49. Muller-Landau, H. *Combined Band Dendrometer Protocol* (ForestGEO/CTFS Global Forest Carbon Research Initiative, 2022); https://forestgeo.si.edu/sites/default/files/panama_dendrometer_protocol_2022-06-06.pdf

50. Forrester, D. I. et al. Generalized biomass and leaf area allometric equations for European tree species incorporating stand structure, tree age and climate. *For. Ecol. Manage.* **396**, 160–175 (2017).
51. Jakubowski, M. & Dobroczyński, M. Allocation of wood density in European oak (*Quercus robur* L.) trees grown under a canopy of Scots pine. *Forests* **12**, 712 (2021).
52. Matula, R., Damborská, L., Nečasová, M., Geršl, M. & Šrámek, M. Measuring biomass and carbon stock in resprouting woody plants. *PLoS ONE* **10**, e0118388 (2015).
53. Phillips, R. P., Ehlitz, Y., Bier, R. & Bernhardt, E. S. New approach for capturing soluble root exudates in forest soils. *Funct. Ecol.* **22**, 990–999 (2008).
54. Norby, R. J. et al. Data from: Enhanced woody biomass production in a mature temperate forest under elevated CO₂ [Dataset]. *Dryad* <https://doi.org/10.5061/dryad.z612jm6jw> (2024).

Acknowledgements

We thank N. Harper and P. Miles for long-term technical support of the FACE facility operations; G. McLean and A. Gardner for shorter-term technical support; P. Blaen and A. Poynter for assistance with initial experimental set-up; H. Begum, A. Kiani, T. Nguyen and H. Warmington for tissue processing; Nuffield Research Placement students, and student and corporate volunteers for assistance with sample processing; and arborists from Rob Keyzor Arboricultural Consultancy for sample retrieval. Funding was provided by the JABBS foundation, the University of Birmingham, and the John Horseman Trust (to A.R.M.), the UK Natural Environmental Research Council through grants NE/S015833/1 (to A.R.M.) and NE/T012323/1 (to S.U.), the UK Research and Innovation Frontier Research Grant QUERCUS funded under EP/X025098/1 (to N.J.L.), and The University of Birmingham Institute for Advanced Studies Distinguished Visiting Fellowship Programme (to R.J.N.).

Author contributions

A.R.M., S.U., A.R.S., I.P.H., K.M.H. and Z.S. designed and administered the experiment. R.J.N. designed the data synthesis and analysis. R.J.N., N.J.L., C.M., A.R.S., M.K.R., K.v.W., M.S.A., D.B., M.E.C., G.D., R.T.G., R.L.H., A.G.J., A.K. and R.M.T. collected data and contributed to analysis. G.C. and D.B. curated data. J.R.L. provided advice on statistical analysis. R.J.N. wrote the manuscript with substantial input from A.R.M., N.J.L., C.M., S.U., A.R.S., M.K.R., I.P.H. and K.v.W. All authors edited and approved the manuscript.

Competing interests

The authors declare no competing interests.

Additional information

Extended data is available for this paper at <https://doi.org/10.1038/s41558-024-02090-3>.

Supplementary information The online version contains supplementary material available at <https://doi.org/10.1038/s41558-024-02090-3>.

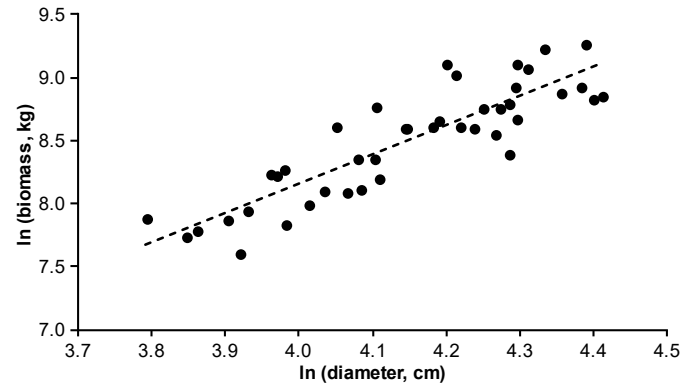
Correspondence and requests for materials should be addressed to Richard J. Norby or A. Robert MacKenzie.

Peer review information *Nature Climate Change* thanks Mingkai Jiang, Ben Bond-Lamberty, Shuli Niu and the other, anonymous, reviewer(s) for their contribution to the peer review of this work.

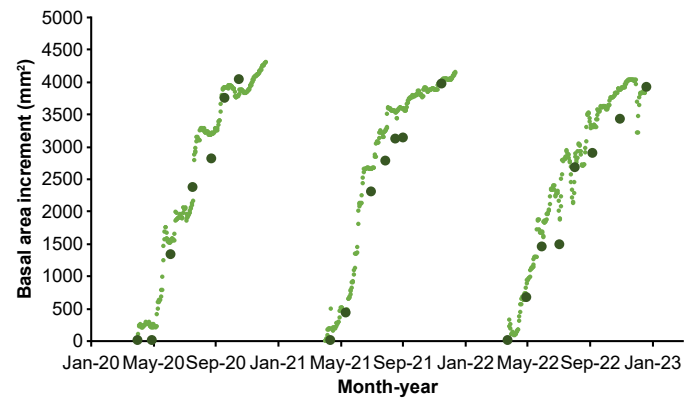
Reprints and permissions information is available at www.nature.com/reprints.



Extended Data Fig. 1 | Aerial view of the BIFoR FACE facility. The research site comprises six experimental arrays of c. 30 m diameter and a flux tower. Photo by Peter Miles, University of Birmingham.

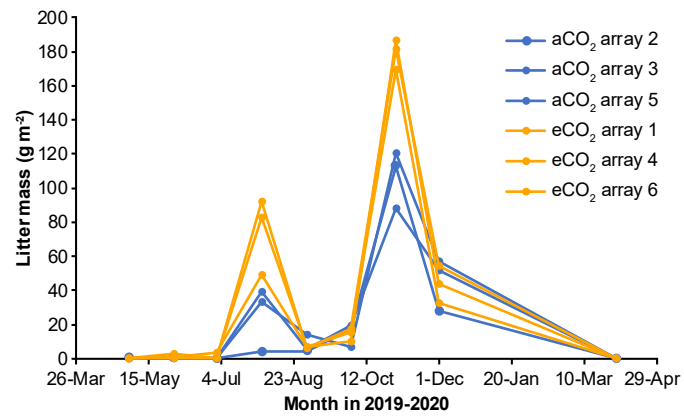


Extended Data Fig. 2 | Allometric relationship between *Quercus robur* tree biomass and tree diameter at breast height. The regression equation is: $\ln(\text{biomass, kg}) = 2.312 \times \ln(\text{diameter, cm}) - 1.0863$; $r^2 = 0.77$. Tree biomass was calculated as tree volume \times wood density of 0.58 g cm^{-3} , with tree volume determined by TLS.

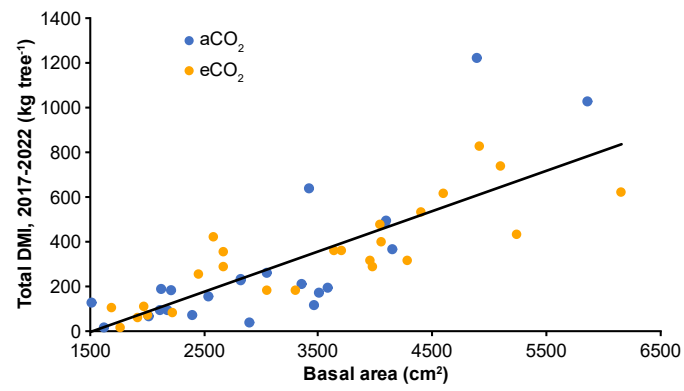


Extended Data Fig. 3 | Comparison of two methods of basal area measurement for a representative tree. The light green dots are calculations based on daily values of circumference from automated dendrometers (Dendrometer increment sensor DRL26A of resolution less than 1 μm ,

Environmental Measuring Systems, Brno, Czech Republic), with the data reset to zero each year. The dark green dots are from similar calculations from monthly surveys of manual band dendrometers as described in Methods.



Extended Data Fig. 4 | Leaf litterfall during 2019. There was substantial leaf loss during the summer, which was greater in elevated CO₂ plots ($P=0.044$, $F_{1,4}=8.36$), prior to the normal autumnal leaf loss (CO₂ effect, $P<0.003$).



Extended Data Fig. 5 | Total dry matter increment per tree, 2017–2022 vs tree basal area in 2018. Blue symbols are ambient CO₂ and orange symbols are elevated CO₂. Regression equation: $DMI = 0.18 \times BAI - 277$; $r^2 = 0.65$.

Reporting Summary

Nature Portfolio wishes to improve the reproducibility of the work that we publish. This form provides structure for consistency and transparency in reporting. For further information on Nature Portfolio policies, see our [Editorial Policies](#) and the [Editorial Policy Checklist](#).

Statistics

For all statistical analyses, confirm that the following items are present in the figure legend, table legend, main text, or Methods section.

- | n/a | Confirmed |
|-------------------------------------|--|
| <input type="checkbox"/> | <input checked="" type="checkbox"/> The exact sample size (n) for each experimental group/condition, given as a discrete number and unit of measurement |
| <input type="checkbox"/> | <input checked="" type="checkbox"/> A statement on whether measurements were taken from distinct samples or whether the same sample was measured repeatedly |
| <input type="checkbox"/> | <input checked="" type="checkbox"/> The statistical test(s) used AND whether they are one- or two-sided
<i>Only common tests should be described solely by name; describe more complex techniques in the Methods section.</i> |
| <input type="checkbox"/> | <input checked="" type="checkbox"/> A description of all covariates tested |
| <input type="checkbox"/> | <input checked="" type="checkbox"/> A description of any assumptions or corrections, such as tests of normality and adjustment for multiple comparisons |
| <input type="checkbox"/> | <input checked="" type="checkbox"/> A full description of the statistical parameters including central tendency (e.g. means) or other basic estimates (e.g. regression coefficient) AND variation (e.g. standard deviation) or associated estimates of uncertainty (e.g. confidence intervals) |
| <input type="checkbox"/> | <input checked="" type="checkbox"/> For null hypothesis testing, the test statistic (e.g. F , t , r) with confidence intervals, effect sizes, degrees of freedom and P value noted
<i>Give P values as exact values whenever suitable.</i> |
| <input checked="" type="checkbox"/> | <input type="checkbox"/> For Bayesian analysis, information on the choice of priors and Markov chain Monte Carlo settings |
| <input checked="" type="checkbox"/> | <input type="checkbox"/> For hierarchical and complex designs, identification of the appropriate level for tests and full reporting of outcomes |
| <input checked="" type="checkbox"/> | <input type="checkbox"/> Estimates of effect sizes (e.g. Cohen's d , Pearson's r), indicating how they were calculated |

Our web collection on [statistics for biologists](#) contains articles on many of the points above.

Software and code

Policy information about [availability of computer code](#)

- | | |
|-----------------|--|
| Data collection | No software was used for data collection |
| Data analysis | Open-source software used in analysis of terrestrial laser scan data (optQSM and TreeQSM) ver. 2.4.1) is described in the Methods. Tree rings were analyzed with TSAPO-Win software (Rinntech, Inc.) |

For manuscripts utilizing custom algorithms or software that are central to the research but not yet described in published literature, software must be made available to editors and reviewers. We strongly encourage code deposition in a community repository (e.g. GitHub). See the Nature Portfolio [guidelines for submitting code & software](#) for further information.

Data

Policy information about [availability of data](#)

All manuscripts must include a [data availability statement](#). This statement should provide the following information, where applicable:

- Accession codes, unique identifiers, or web links for publicly available datasets
- A description of any restrictions on data availability
- For clinical datasets or third party data, please ensure that the statement adheres to our [policy](#)

All data will be publicly available without restriction at Dryad (10.5061/dryad.z612jm6jw)

Human research participants

Policy information about [studies involving human research participants and Sex and Gender in Research](#).

Reporting on sex and gender	<i>Use the terms sex (biological attribute) and gender (shaped by social and cultural circumstances) carefully in order to avoid confusing both terms. Indicate if findings apply to only one sex or gender; describe whether sex and gender were considered in study design whether sex and/or gender was determined based on self-reporting or assigned and methods used. Provide in the source data disaggregated sex and gender data where this information has been collected, and consent has been obtained for sharing of individual-level data; provide overall numbers in this Reporting Summary. Please state if this information has not been collected. Report sex- and gender-based analyses where performed, justify reasons for lack of sex- and gender-based analysis.</i>
Population characteristics	<i>Describe the covariate-relevant population characteristics of the human research participants (e.g. age, genotypic information, past and current diagnosis and treatment categories). If you filled out the behavioural & social sciences study design questions and have nothing to add here, write "See above."</i>
Recruitment	<i>Describe how participants were recruited. Outline any potential self-selection bias or other biases that may be present and how these are likely to impact results.</i>
Ethics oversight	<i>Identify the organization(s) that approved the study protocol.</i>

Note that full information on the approval of the study protocol must also be provided in the manuscript.

Field-specific reporting

Please select the one below that is the best fit for your research. If you are not sure, read the appropriate sections before making your selection.

Life sciences Behavioural & social sciences Ecological, evolutionary & environmental sciences

For a reference copy of the document with all sections, see [nature.com/documents/nr-reporting-summary-flat.pdf](https://www.nature.com/documents/nr-reporting-summary-flat.pdf)

Ecological, evolutionary & environmental sciences study design

All studies must disclose on these points even when the disclosure is negative.

Study description	The FACE facility comprises six experimental arrays surrounding plots of approximately 30 m diameter. CO ₂ -enriched air (1-2% by volume) is released from vertical vent pipes in three of the arrays to attain a target CO ₂ concentration at plot center that is 150 ppm above ambient CO ₂ .
Research sample	The study site is a deciduous forest dominated by 180-year old <i>Quercus robur</i> L. trees, which represent 92% of the forest's basal area. The forest canopy is 24-26 m high with a leaf area index of the overstory of about 6. The forest understory comprises <i>Corylus avellana</i> L. coppice, <i>Acer pseudoplatanus</i> L., <i>Crataegus monogyna</i> Jacq., and a few individuals of other broadleaf species.
Sampling strategy	All trees with dbh>10 cm within the defined plts were measured. Leaf litter was collected in 2 or 3 traps per plot (201-2020) and 6 traps per plot (2020-2022). Fine-root production was measured in 5 in-growth cores per plot.
Data collection	Dendrobands were measured by MEC and AGJ (2016-2018), RJN and CM (2019) and RTG (2020-2023). TLS data were collected by KVV. Tree rings were collected by NJL and CM and analyzed by NJL. Exudation was measured by MKR. Litter was collected by DB. Fine root were measured by ARS and AK
Timing and spatial scale	Dendrobands were measured approximately monthly between April and December. TLS scan was done in in January and February 2022. Tree rings were collected in June 2021 and August 2022. Litter was collected monthly from March-October and weekly from mid-October to mid-December. Exudation was measured in August and November 2020 and March and June 2021. Fine root in-growth cores were processed on 4/27/21, 9/7/21, 1/18/22, 5/9/22, 9/12/22, and 1/23/23.
Data exclusions	No data were excluded
Reproducibility	The experiment cannot be repeated.
Randomization	CO ₂ treatments were randomly assigned to the experimental plots, which were laid out without bias. Tree growth per plot after CO ₂ treatment was initiated was normalized to pretreatment differences based on average basal area increment from 2011-2015 from tree ring analysis.
Blinding	Blinding was not possible because the data were collected in the plots with defined treatments.
Did the study involve field work?	<input checked="" type="checkbox"/> Yes <input type="checkbox"/> No

Field work, collection and transport

Field conditions	The site is accessible by road, PPE is required for all researchers, and buildings on site provide protection from adverse weather. Mean annual maximum and minimum temperatures (1991 – 2020) were 13.5 and 6.0 °C with 676 mm precipitation.
Location	central England: 52.801°N, 2.301°W
Access & import/export	Leaf, root, and soil samples are maintained on site or at the University of Birmingham.
Disturbance	FACE facility construction was engineered to minimize tree removal. No vegetation is removed from the experimental plots and soil sampling is confined to defined locations.

Reporting for specific materials, systems and methods

We require information from authors about some types of materials, experimental systems and methods used in many studies. Here, indicate whether each material, system or method listed is relevant to your study. If you are not sure if a list item applies to your research, read the appropriate section before selecting a response.

Materials & experimental systems

n/a	Involvement in the study
<input checked="" type="checkbox"/>	<input type="checkbox"/> Antibodies
<input checked="" type="checkbox"/>	<input type="checkbox"/> Eukaryotic cell lines
<input checked="" type="checkbox"/>	<input type="checkbox"/> Palaeontology and archaeology
<input checked="" type="checkbox"/>	<input type="checkbox"/> Animals and other organisms
<input checked="" type="checkbox"/>	<input type="checkbox"/> Clinical data
<input checked="" type="checkbox"/>	<input type="checkbox"/> Dual use research of concern

Methods

n/a	Involvement in the study
<input checked="" type="checkbox"/>	<input type="checkbox"/> ChIP-seq
<input checked="" type="checkbox"/>	<input type="checkbox"/> Flow cytometry
<input checked="" type="checkbox"/>	<input type="checkbox"/> MRI-based neuroimaging